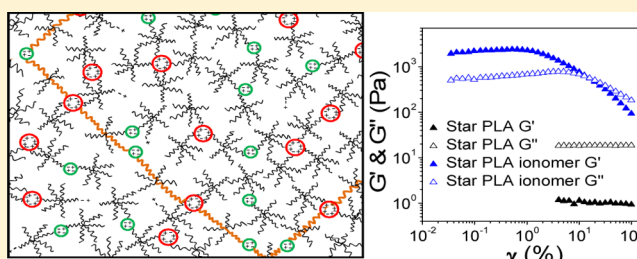


## Star Telechelic Poly(L-lactide) Ionomers

Amruta Kulkarni,<sup>†</sup> Ashish Lele,<sup>\*,†</sup> Swaminathan Sivaram,<sup>‡</sup> P. R. Rajamohanam,<sup>†</sup> Sachin Velankar,<sup>§</sup> and Apratim Chatterji<sup>||</sup><sup>†</sup>Academy of Scientific and Innovative Research, CSIR-National Chemical Laboratory, Pune, 411008, India<sup>‡</sup>CSIR-National Chemical Laboratory, Pune, 411008, India<sup>§</sup>Chemical Engineering Department, University of Pittsburgh, Pittsburgh, Pennsylvania 15261, United States<sup>||</sup>Physics Department, Indian Institute of Science Education and Research, Pune, 411008, India

## Supporting Information

**ABSTRACT:** Poly(L-lactide) (PLA), a biodegradable and biorenewable polymer, has many excellent properties that are equivalent to those of petroleum-derived plastics such as polystyrene, aromatic polyesters, etc. However, a major disadvantage of PLA which limits its processability is its poor melt elasticity. In this work we explore the possibility of improving the viscoelastic properties of PLA melt by incorporating ionic groups on the polymer. Specifically, we demonstrate the synthesis of star telechelic PLA anionomers by a three-step procedure involving synthesis of Star PLA, converting the hydroxyl end groups into carboxylic acid end groups, and finally converting these into ionic groups. Rheology data showed a dramatic increase in the elasticity of the star telechelic ionomer melts relative to the Star PLA melts. The viscoelasticity of star telechelic ionomers melts could be modulated by varying the number of ionic groups per molecule.



## INTRODUCTION

Plastics derived from petroleum are ubiquitous in everyday life. However, the increasing cost of crude oil and greater awareness about the harmful environmental effects of plastic waste are fueling the development of new biodegradable and/or biorenewable plastics. One such material, poly(L-lactide) (PLA), is now commercially manufactured and is available at a competitive price for conversion into products. Several physical properties of PLA are equivalent to those of petroleum derived commodity plastics such as polystyrene.<sup>1–3</sup> PLA can also be processed using conventional polymer processing equipment. However, a major deficiency that limits the processability of PLA is its poor melt strength, which causes problems such as sagging, necking, and nonuniform draw down during thermoforming, blown film extrusion, film and sheet extrusion, and foaming operations.<sup>2–7</sup> Strategies for improving the melt strength of PLA reported so far in the literature include incorporation of long chain branches on PLA<sup>8–12</sup> and mixing nanofibrous fillers in PLA.<sup>13–17</sup> The first approach involves reactive extrusion of PLA with certain peroxides or multifunctional branching agents, resulting in branching accompanied by the formation of undesirable microgels. The challenges in the second approach pertain to achieving uniform filler dispersion and using thermally stable biodegradable fillers.

A plausible new approach to improve the melt elasticity of PLA is to convert it into an ionomer. Ionomers are polymers containing small amounts (up to 15 mol %) of ionic groups, which associate to form nanometer-sized clusters because of micro phase separation from the dielectric medium of the

polymer.<sup>18</sup> The formation of ionic clusters, as elucidated by small-angle X-ray scattering experiments, depends on various factors, such as concentration of ionic groups, type of counterion, process of incorporation of ions in the chain, and thermal treatment.<sup>19–23</sup> The characteristic microstructure of ionomers often results in profound modification of the properties of the polymer relative to the nonionic state, and this is the primary reason for the considerable interest in this class of polymers.<sup>24–27</sup> For instance, incorporation of a small number of ionic groups on the polymer chains restricts their mobility and hence results in an increased glass transition temperature ( $T_g$ ).<sup>25,27–31</sup> Similarly, the hindered mobility of polymer chains broadens the melting transition.<sup>25,32,33</sup> Such modulations of the physical properties of ionomers have recently been used to demonstrate shape memory and self-healing.<sup>26,32,34</sup>

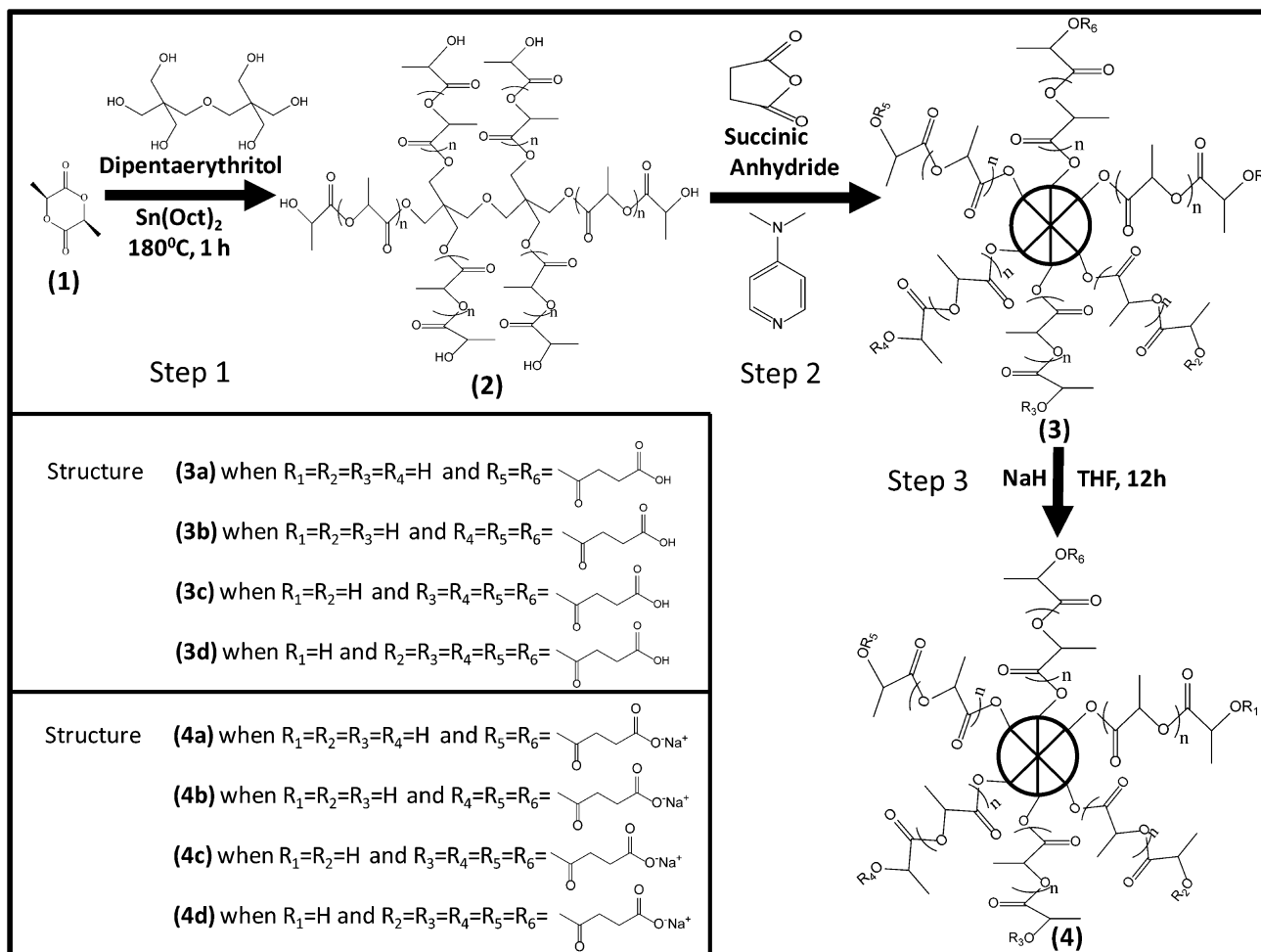
Coulombic interactions of the ionic groups in an ionomer are sustained even at high temperatures. Consequently, ionomers often exhibit unusual melt flow properties such as shear-thickening<sup>35</sup> and are therefore thought to be useful as rheology modifiers.<sup>36</sup> The rheological properties of ionomers have been well studied,<sup>37–40</sup> and correlations between viscosity and ion type and between viscosity and ionomer concentration are known.<sup>41</sup> Greener et al.<sup>42</sup> observed a significant and systematic increase in the melt viscosity, plateau modulus, and flow

Received: August 21, 2015

Revised: August 25, 2015

Published: September 9, 2015

**Scheme 1.** Reaction Scheme for Synthesis of Six Arm Star PLA (2) by Ring Opening Polymerization of L-Lactide (1) in the Presence of Dipentaerythritol; Six Arm Star PLA Acid (3) by Acidification of the Hydroxyl End Functional Groups of Star PLA (2); and Six Arm Star PLA Ionomer (4) by Neutralization of Star PLA Acid (3) in the Presence of Sodium Hydride<sup>42</sup>



<sup>42</sup>Structures of compounds (3a–d) and ionomers (4a–d) are explained.

activation energy of polyester ionomers melts on addition of ionic groups to polymer. Weiss et al.<sup>41,43,44</sup> studied the linear rheology of lightly sulfonated polystyrene ionomers. They showed that at very low sulfonic group concentration (one and two sulfonic groups per chain) the ionomers have significantly higher melt viscosity than the precursor polymer. The flow activation energy of these low molecular weight ionomers was similar to that of a high molecular weight precursor, whereas the characteristic relaxation time of the ionomers was found to be considerably greater than the relaxation time of the precursor polymers. Stadler et al.<sup>45</sup> observed the existence of time dependent terminal relaxation in the linear viscoelastic rheology of the linear telechelic polybutadiene ionomer. Qiao et al.<sup>46</sup> studied the nonlinear rheology of lightly sulfonated polystyrene ionomers under oscillatory shear, steady shear, and shear start-up experiments. The nanodomain microstructure of ionomers was found to govern changes in viscosity and elasticity under large deformation flows. Extensional rheological properties of ionomers have also been studied by a few researchers.<sup>47–49</sup>

Of the two main types of ionomers, namely random ionomers, in which the ions are located randomly along the chain, and telechelic ionomers, in which the ions are placed at

the chain ends, the latter are better model systems to study structure–property relations because of the possibility of having precise control of the molecular weight between ionic clusters.<sup>50</sup> The other important structural parameter for ionomers is the number of ionic groups on a molecule. For telechelic ionomers, it is possible to increase the number of ionic groups per molecule by starting with star polymers such that the maximum number of ionic groups on the polymer is equal to the number of star arms. There are only a few reports on star telechelic ionomers. Fetters et al.<sup>51</sup> studied the melt rheology of star telechelic polyisoprenes with different ionic groups. They compared the viscoelastic behavior of mono-telechelic ionomers, which assembled into star conformations, with the viscoelastic properties of star precursors and found that the melt viscosities of ionomers were much too high to be explained by the rheological models for star polymers. Bagrodia et al.<sup>52,53</sup> synthesized three-arm star polyisobutylene ionomers and observed an increase in the  $T_g$  and melt viscosity for these ionomers relative to the nonionic counterpart. Indeed, the introduction of sulfonic acid groups qualitatively changed the viscous polyisobutylene liquid into an elastomeric material at room temperature. van Ruymbeke et al.<sup>54</sup> investigated the linear viscoelastic behavior of the linear and star telechelic

polyisoprene melts. They showed theoretically and experimentally that the relaxation and dynamics of polymer chains was greatly affected by ionic associations. To the best of our knowledge, there are only two reports<sup>55,56</sup> on PLA ionomers so far, and both are based on linear chains. Ro et al.<sup>55,56</sup> synthesized telechelic and random chain PLA ionomers and investigated their thermal and mechanical properties.

In this paper we report on the synthesis of star telechelic PLA ionomers and their structural elucidation by NMR and FTIR. We show the effect of ionic associations on the thermal properties and the linear viscoelastic rheological properties of the Star PLA ionomers.

## EXPERIMENTAL SECTION

**Materials.** L-Lactide monomer was purchased from Purac Asia Pacific Pte Ltd. (Singapore). Dipentaerithritol (DPE), pentaerithritol (PE), tripentaerithritol (TPE), stannous 2-ethylhexanoate (SnOct<sub>2</sub>), succinic anhydride, dimethylaminopyridine (DMAP) and sodium hydride (NaH, 55% dispersion in mineral oil) were purchased from Sigma-Aldrich (India) and were used as received. Toluene (HPLC grade), chloroform (GR grade), methanol (GR grade) and tetrahydrofuran (THF, GR grade) were purchased from Merck India. Solvents toluene and THF were distilled and rigorously dried before use. THF was passed over P<sub>2</sub>O<sub>5</sub> and activated alumina and then distilled over sodium metal under nitrogen atmosphere for 4 h before use. All glassware was dried at 60 °C in vacuum oven for 24 h before reactions.

**Synthesis of Six-arm Star PLA (2).** Ring opening melt polymerization (Scheme 1, Step 1) was carried out in glass ampules with sealable necks. 1 wt %/vol% stock solution of catalyst was prepared in distilled dry toluene. The monomer to initiator molar ratio was taken as 69.4:1 so that the targeted overall molecular weight of the Star PLA would be 10 000 g/mol. Dipentaerithritol was used as an initiator to produce six-arm Star PLA (2), and the initiator to catalyst molar ratio was fixed at 167:1. L-lactide (1) 20 g (0.139 mol) of, 0.508 g (0.002 mol) of DPE and 3 mL (0.000072 mol) of SnOct<sub>2</sub> stock solution were transferred into glass ampule inside a glovebox. The contents in the ampule were held at 55 °C for 4 h under vacuum to remove toluene and the ampule was heat-sealed under vacuum. Polymerization was carried out in an oven at 180 °C for about 1 h. The polymer was dissolved in chloroform and precipitated in methanol thrice, and finally filtered to remove unreacted products. The purified polymer (2) was dried in a vacuum oven for 24 h at 60 °C.

**Synthesis of Star PLA Acid (3b).** Six-arm Star PLA (2) having –OH end groups 14 g (0.0084 mol) was dissolved in 70 mL of distilled dry THF at 45 °C in a two-neck flask under nitrogen atmosphere and the solution was cooled down to room temperature. Succinic anhydride 4.2 g (0.042 mol, 5 times excess on molar basis) and 1.0248 g (0.0084 mol) DMAP were dissolved in 70 mL of dry THF in another two-neck flask at 0 °C and after stirring for about 30 min the polymer solution was added dropwise to this solution using a syringe. All of these processes were carried out under nitrogen atmosphere using a Schlenk line. The reaction (Scheme 1, Step 2) was carried out at room temperature under nitrogen atmosphere for 6 h. The polymer was precipitated in methanol thrice, filtered and dried in vacuum oven for 24 h at 60 °C. The Star PLA having an average of 2, 3, 4, and 5 acid end groups (3a–d) were prepared using reaction time varying between 0 to 12 h keeping other parameters same.

**Synthesis of Star PLA Ionomer (4b).** Star PLA acid (3b) 12.5 g (0.0075 mol) was dissolved in 125 mL dry THF at 50 °C in a two-neck flask under nitrogen atmosphere. After the polymer was completely dissolved in THF, the solution was cooled down to room temperature and 0.509 g (0.01125 mol, 1.5 times molar excess) NaH was added to the polymer solution. The reaction (Scheme 1, Step 3) was carried out at room temperature for 12 h. After the reaction, the THF was evaporated and the product dried at 60 °C in vacuum oven. The polymer was washed with dried pet-ether. Star PLA

ionomers with different numbers of ionic end groups (4a,c,d) were similarly prepared starting from their respective Star PLA acid polymers (3a,c,d).

**Characterization.** Fourier Transform Infrared Spectroscopy (PerkinElmer Spectrum GX FTIR) measurements were done using KBr pellets containing the PLA samples. 128 FTIR scans were obtained at 2 cm<sup>-1</sup> resolution and the data added to give the infrared spectrum. Nuclear Magnetic Resonance (NMR) experiments were done on Bruker 400 Ultrashield instrument. 10 mg/μL concentration solutions of samples in deuterated chloroform (Sigma-Aldrich 99.8 atom % D) were prepared. Twenty thousand scans were collected for quantitative analysis. Trimethylsilane was used as a reference. Areas under <sup>1</sup>H and <sup>13</sup>C NMR peaks were calculated using ACD spectral viewer software. The peak positions in the <sup>13</sup>C spectra were assigned using chloroform as the reference. Thermal measurements were done using a Differential Scanning Calorimeter (DSC, TA Instruments Q100) under nitrogen flow of 50 mL/min. The DSC was calibrated using Indium standard. 5–7 mg samples were crimped in aluminum pans and heated to 200 °C at 5 °C/min. The samples were cooled down to 0 °C and second heat scans were obtained by heating to 200 °C at the same rate. Heats of crystallization and melting were calculated respectively from the cooling and second heating scans using TA universal analysis software. Rheological measurements were performed on an ARES rheometer (TA Instruments). Polymer powder was placed on 25 mm parallel plate, melted at 150 °C under nitrogen atmosphere and compressed by setting the gap (0.4 mm) between the plates. Strain sweep experiments were carried out at 150 °C and 10 rad/s frequency. Frequency sweeps were carried out at the same temperature at 0.4% to 10% strain, which were in the linear viscoelastic regime.

## RESULTS AND DISCUSSION

**Structural Elucidation of Star PLA Ionomer.** In the first step of preparation of Star PLA ionomer, ring opening polymerization (ROP) of L-lactide was performed in melt in the presence of stannous 2-ethylhexanoate and DPE. The polymerization proceeds by a coordination insertion mechanism in which the monomers get affixed to the six initiating sites of DPE, resulting in a six arm Star PLA (2) via the core first approach. Figure 1 shows the structure of the six-arm Star PLA (2) and its proton NMR spectrum. The peaks in the <sup>1</sup>H NMR spectrum were assigned keeping in mind the structure of the Star PLA (2), and the area under each assigned peak was

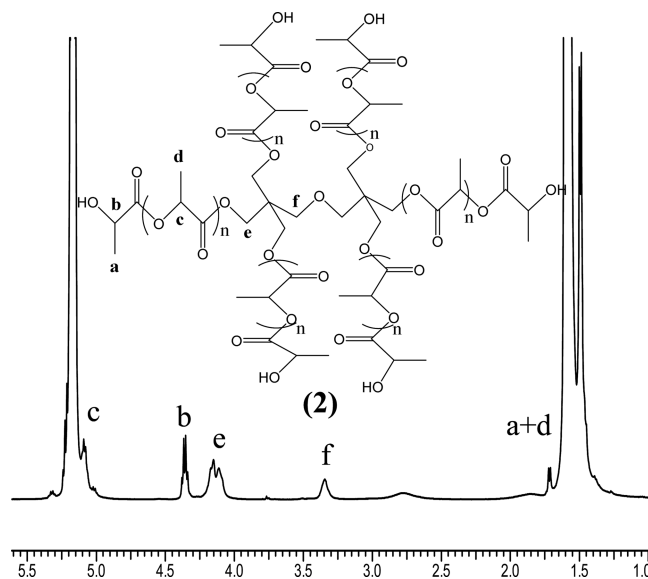


Figure 1. <sup>1</sup>H NMR and structure of Star PLA (2).

calculated. The area under peak **b** [methine ( $-\text{CH}-$ ) proton] appearing at 4.5 ppm was taken as 6, since there are six end groups per molecule. The areas of all other peak were calculated relative to peak **b**. Peaks **f** and **e** at 3.35 and 4.2 ppm respectively correspond to the methylene protons ( $-\text{CH}_2-$ ) of the DPE initiator; the areas under these peaks confirm that all the initiating sites of DPE have participated in the reaction, resulting in six arms of the star architecture. The ratio of protons **c**:**b** also confirms that the molecular weight of the Star PLA (**2**) was close to the theoretically expected molecular weight. Since all the initiating sites are chemically equivalent and equally accessible, they will polymerize by the same propagation rate  $k_p$ . Hence, it is likely that the molecular weight of each of the 6 arms is the same.

In the second step of the synthesis procedure, the Star PLA (**2**) was dissolved in dry THF and its  $-\text{OH}$  end groups were reacted with succinic anhydride in the presence of the nucleophilic catalyst DMAP. The choice of the solvent was critical to the success of this reaction. THF was chosen based on the work of Danko et al.,<sup>57</sup> who studied the conformation of Star PLA having different numbers of arms ranging from 2 to 6 in this solvent. They noticed that Star PLA having 4–6 arms adopts stretched conformations in which the end groups of polymer are away from the core. This suggests that the end groups are exposed and, therefore, more accessible for reaction with succinic anhydride.

Figure 2 shows the  $^1\text{H}$  NMR spectrum of the Star PLA acid (**3**) that is isolated and purified after reaction with succinic

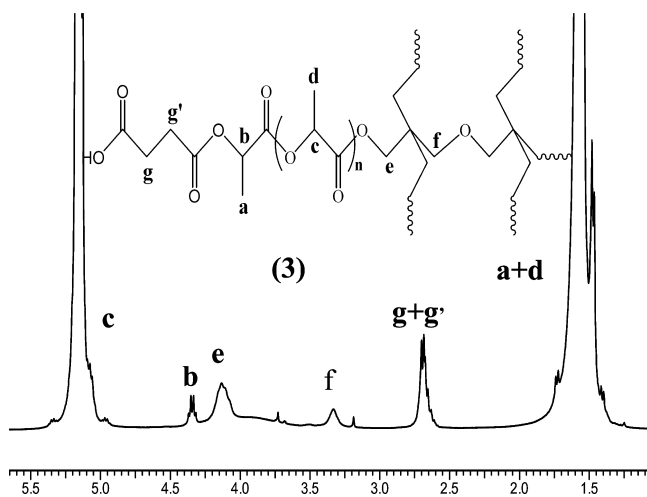


Figure 2.  $^1\text{H}$  NMR and structure of Star PLA acid (**3**).

anhydride. The peaks **g**+**g'** at 2.7 ppm correspond to the ethylene protons of the reacted succinic acid. Table 1 shows a comparison of the theoretically expected and experimentally determined peak areas normalized by the area under peak **c** coming from the repeat unit of PLA. The theoretical peak areas are calculated assuming that all six  $-\text{OH}$  end groups of the Star PLA are converted into  $-\text{COOH}$  end groups after reaction with succinic anhydride. Therefore, for the case of Star PLA acid, the differences between the theoretical and experimental ratios of peak areas for **b**:**c** and (**g**+**g'**):**c** indicate that in fact only three of the six arms have been converted to acid end groups. The other ratios are in close agreement with theoretical calculations. Noting that methanol was used for precipitation and purification of the polymer, the small peaks at 3.7 and 3.4 ppm are assigned to the methoxy ester of succinic acid, which is

formed by reaction of methanol with the excess succinic anhydride in the presence of DMAP. This was confirmed by separately synthesizing the ester under similar reaction conditions.

The carboxyl end functionalization of Star PLA (**2**) by succinic anhydride and the extent of reaction can also be confirmed by the  $^{13}\text{C}$  NMR spectra shown in Figure S5 in the Supporting Information. A detailed explanation is also provided in the Supporting Information with Figure S5.

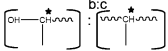
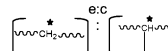
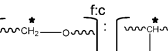
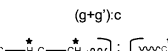
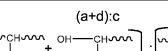
It was found that the number of acid end groups per mole of DPE can be varied as a function of reaction time. Shorter reaction time led to fewer arms having acid end groups. In this manner, polymers having an average of 2, 3, 4, and 5 acid end groups (**3a–d**) were prepared using reaction time varying between 0 and 12 h (see Figure S3 and Figure S4 in the Supporting Information).

In the third step of the synthesis procedure, the Star PLA acid (**3**) was reacted with NaH in dry THF. NaH is a strong non-nucleophilic base which deprotonates the acid functional groups without cleaving the ester repeat unit. Upon formation of the carboxylate ion, the electronic environment around the carbon of the carboxylate ion changes because of delocalization of the electron cloud and consequent deshielding of the carbon nucleus. The electronic environments of the carbon atoms next to the carboxylate group along the chain are also affected. Figure 3 shows two regions of the  $^{13}\text{C}$  NMR spectra of Star PLA acid (**3**) and Star PLA ionomer (**4**). The corresponding structures and peak assignments are also shown. The peaks corresponding to the carbon of the methylene group **j**, **j'** and the carbon of the carboxyl group **k** are affected by the presence of the ion. In particular, the downfield shift of peak **j** by  $\sim 1.5$  ppm substantiates ionomer formation. Quantification of the extent of neutralization could not be done from the  $^{13}\text{C}$  spectra because of poorly resolved signals.

We show in Figure 4 the FT-IR spectra for all three samples, Star PLA (**2**), Star PLA acid (**3b**), and Star PLA ionomer (**4b**). The fingerprinting peaks for PLA repeat units such as the  $\text{C}=\text{O}$  stretch at  $1760$ , the  $\text{CH}_3$  bending and stretching at  $1450$  and  $2950$   $\text{cm}^{-1}$  (not shown), and the  $\text{O}-\text{C}=\text{O}$  stretching at  $1190$   $\text{cm}^{-1}$  to  $1090$   $\text{cm}^{-1}$  are seen for all three polymers. The FTIR spectra for the Star PLA (**2**) and Star PLA acid (**3b**) are indistinguishable even though their end groups are different. This is probably because the carboxylic acid groups in the Star PLA acid (**3b**) are not H-bonded and therefore do not show a peak at the characteristic wavenumber of  $1700$   $\text{cm}^{-1}$  in the spectrum. Also, the absorbance of non-H-bonded acid end groups, which should appear at  $1750$   $\text{cm}^{-1}$ , is likely merged with the dominant absorbance of the ester at  $1760$   $\text{cm}^{-1}$  and therefore not resolved. In contrast, the Star PLA ionomer (**4b**) shows a distinct new peak for the  $\text{C}=\text{O}$  asymmetric stretch of metal carboxylate at  $1600$   $\text{cm}^{-1}$ .<sup>56,58</sup> This reconfirms the formation of the ionomer end group. Quantitative estimation of the number of ionic groups was not possible from the spectrum; however, the specificity and high reactivity of NaH with acid groups is likely to result in conversion of all carboxylic acid end groups into carboxylate ions.

**Microstructure of Star Ionomer Melt.** The elucidation of the molecular structure of Star PLA-ionomer (**4b**) presented above suggests that the ionomer contains two types of polymer chains: those that have ionic end groups ( $\text{COO}^-\text{Na}^+$ ) and those that have nonionic ( $\text{CH}_2-\text{OH}$ ) end groups. On average, the fraction of these two species is equal in the as-synthesized six-arm Star PLA ionomer (**4b**). The telechelic ionomer chains

Table 1. Structural Elucidation by NMR of Star PLA (2) and Star PLA Acid (3b)

Peak ratios	Theoretical expected ratios for star PLA (2) <sup>a</sup>	Experimentally determined ratios for star PLA (2) <sup>b</sup>	Theoretical expected ratios for star PLA acid (3)	Experimentally determined ratios for star PLA acid (3)
	6/138 = 0.043	6/139 = 0.043	0/138 = 0	2.5/138 = 0.018
	12/138 = 0.086	10.1/139 = 0.072	12/138 = 0.086	11.54/139 = 0.079
	4/138 = 0.028	3.5/139 = 0.025	4/138 = 0.028	3.64/139 = 0.026
	0/138 = 0	0/139 = 0	(4*6)/138 = 0.173	15.40/139 = 0.110
	(3*138 + 6*3) / 138 = 3.130	460/139 = 3.309	(3*138 + 6*3) / 38 = 3.130	447/139 = 3.215

<sup>a</sup>Theoretical number of repeat units = 138 (calculated from mole ratio of monomer to initiator taken for polymerization). <sup>b</sup>Experimental number of repeat units = 139 (calculated from the area under peak c of the repeat unit with respect to the area under peak b, which was taken as 6).

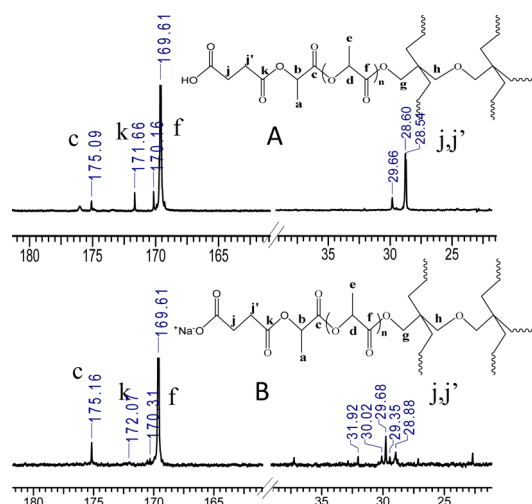


Figure 3. <sup>13</sup>C NMR spectra for (A) Star PLA acid (3) and (B) Star PLA ionomer (4).

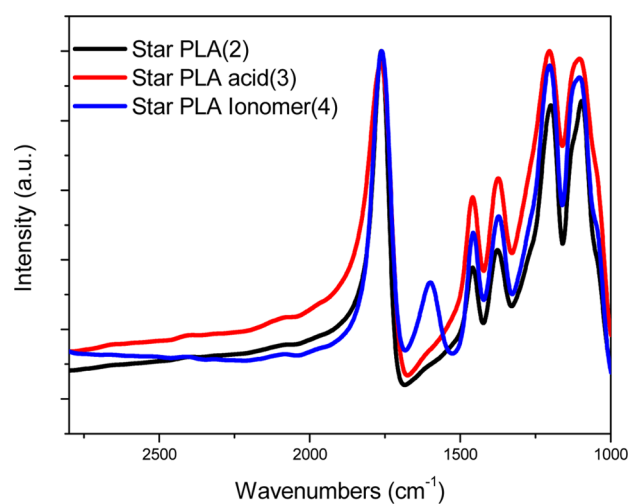
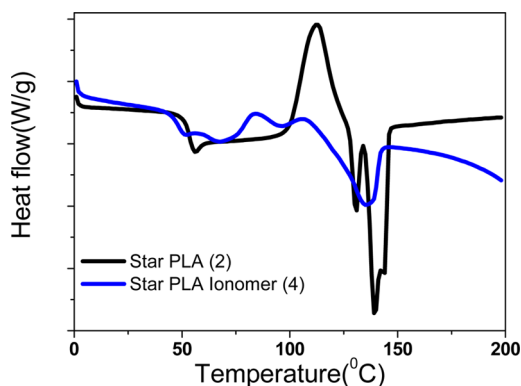


Figure 4. FT-IR spectra for Star PLA (2), Star PLA acid (3b), and Star PLA ionomer (4b).

are likely to associate through dipolar interactions of the ionic groups to form clusters. The propensity to form interconnected clusters can be expected to be higher for star ionomers containing larger number of ionic end groups. PLA chains that

are part of this network structure are expected to be elastically active and thereby have the ability to bear significant mechanical stress. The ionic associations can be expected to hinder the mobility of star arms.

**Thermal and Rheological Properties of Star PLA Ionomers.** The second heat DSC scans for Star PLA (2) and Star PLA-ionomer (4b) are shown in Figure 5. PLA is



**Figure 5.** DSC second heat for Star PLA (2) and Star PLA ionomer (4).

known to have slow crystallization kinetics. In addition there are six end groups in each Star PLA molecule, which act as defects that hinder crystallization. As a result, none of the PLA samples showed crystallization exotherm in the cooling scans (data not shown). Also, due to the low molecular weight of the Star PLA used in this work, the peak melting point of these polymers is lower than the typical melting point of  $\sim 170$  °C for a high molecular weight linear PLA.

In the second heating scan, the PLA samples showed a glass transition followed by a cold-crystallization exotherm and finally the melting endotherm. The multiple peaks of the melting endotherm are a result of the formation of imperfect crystals during cold crystallization, which melt during heating, recrystallize, and remelt at a higher temperature. It is worth noting that the Star PLA ionomer shows a melting endotherm over a wider temperature range of 115–150 °C in comparison with the melting endotherm of the Star PLA (124–150 °C). This suggests a broad crystallite size distribution for the Star PLA ionomer (4b) relative to the Star PLA (2). Further, the heat of fusion of the crystallites in the Star PLA ionomer (4b) is lower than that in the Star PLA (Table 2), indicating relatively

**Table 2.** DSC Results for Star PLA (2) and Star PLA Ionomer (4)

Sample	$\Delta H_f$ (J/g)	$\Delta H_{cc}$ (J/g)	$T_g$ (°C)	$T_c$ (°C)	$T_m$ (°C)
Star PLA (2)	32.7	28.2	51.4	112.4	130; 139
Star PLA ionomer (4)	15.8	12	48; 63	83; 105	134

lower degree of crystallinity in the ionomer. The broader crystallite size distribution and lower degree of crystallinity in the ionomer is most likely the result of hindered mobility of polymer chains due to associations of ionic end groups. Dolog and Weiss have reported similar observations for polyethylene ionomer.<sup>32</sup> Reduced crystallinity of ionomers has also been reported by other researchers.<sup>25,30,33,63</sup>

While the Star PLA (2) showed one  $T_g$ , the Star PLA-ionomer (4) showed two glass transition temperatures, as can be seen in Figure 5. The presence of two  $T_g$ 's in the Star PLA ionomer is also supported by modulated DSC experiment (Figure S1 of the Supporting Information) and DSC heating

scan after isothermal melt crystallization of the polymer (Figure S2 of the Supporting Information). One likely reason for the two  $T_g$ 's seen in the ionomer could be that the sample contains two types of polymer chains: those that contain ionic end groups, which are associated in ionic clusters and therefore have hindered mobility resulting in a higher  $T_g$ , and those that have nonionic end groups, which are not tethered to any cluster and hence have a lower  $T_g$ . Another possible reason for the two glass transitions of the ionomer could be that there are two types of aggregates in the ionomer: (i) multiplets, which are formed by aggregation of only the ionic pendent entities, and (ii) clusters, which are formed when the ionic content is high, and comprise several multiplets that include the hydrocarbons polymer chains within the aggregates.<sup>25,28,29,31</sup> The glass transition temperature of the ionomer that contains multiplets is lower than the  $T_g$  of the ionomers that contain clusters. This is because the mobility of polymer chains inside the clusters is highly restricted. It is not clear which of these two possibilities results in the two glass transition temperatures observed for the Star PLA-ionomer. However, either way, the chain mobility is hindered. The lower  $T_g$  of the Star PLA ionomer (Table 2) is slightly lower (by  $\sim 3$  °C) than the  $T_g$  of the Star PLA. The reason for this is not entirely clear.

Results of strain sweep oscillatory rheology performed at 10 rad/s at 150 °C can be seen in Figure 6. The storage modulus

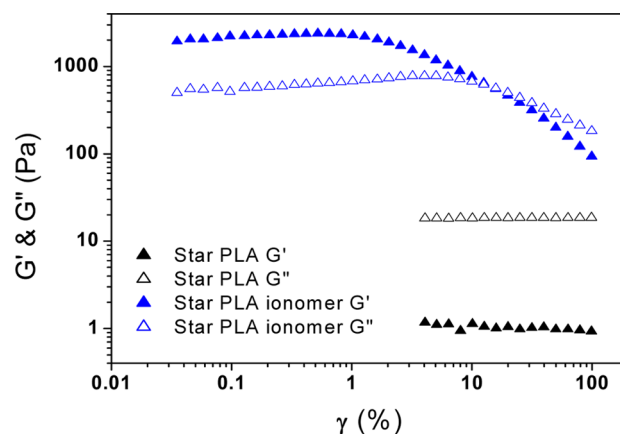


**Figure 6.** Strain sweep for Star PLA (2) and Star PLA ionomer (4b) at temperature 150 °C and frequency 10 rad/s.

( $G'$ ) and the loss modulus ( $G''$ ) are plotted as a function of strain (%) for Star PLA (2) and Star PLA ionomer (4). The Star PLA (2) melt shows a predominantly viscous response in which  $G'' > G'$  and both are independent of strain. However, the Star PLA ionomer (4) melt shows qualitatively and quantitatively different rheological behavior. Here,  $G' > G''$  at low strains, indicating a dominantly elastic response, and both moduli are significantly higher than the moduli of the Star PLA (2) melt. With increasing strain, the melt transitions from linear to nonlinear region, in which the  $G''$  increases, reaches a maximum, and then crosses the  $G'$ . This indicates that the elastic structure at low strains yields at high strain to form a viscous fluid.<sup>64</sup> The value of  $G'$  of Star PLA ionomer (4) melt is higher than that of Star PLA (2) melt by at least 3 orders of magnitude. This increase in the elastic modulus is an indication of the existence of a network structure. We presume that the ionic aggregates are transient in nature, since the ions can hop from one cluster to another at high temperatures or at high

shear stresses. This results in a viscous response at long times and/or at high stresses.

The frequency sweep data for these samples is shown in Figure 7. The Star PLA (2) melt showed predominantly viscous

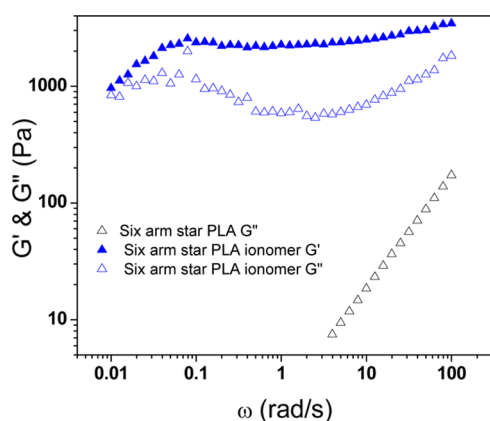


**Figure 7.** Frequency sweep for Star PLA (2) and Star PLA ionomer (4b) at temperature 150 °C.

behavior ( $G'' \gg G'$ ,  $G'' \sim \omega$ ,  $G'$  data not shown). In contrast, the Star PLA ionomer (4) melt showed a predominantly elastic response in which  $G' > G''$ ,  $G'$  had a weak frequency dependence,  $G''$  showed a shallow minimum, and a hint of a crossover frequency was seen at the lowest probed frequency, indicating a long characteristic relaxation time of the order of 100 s. This data also supports the existence of a transient network possibly formed by ionic interactions.

The density of elastically active chains estimated from the value of the plateau modulus ( $G_0 \approx \nu RT$ ) turns out to be a low value of about  $\nu = 0.5 \text{ g mol}^{-3}$ . Here, the value of the plateau modulus  $G_0$  is taken approximately as the value of  $G'$  at the frequency ( $\sim 2 \text{ rad/s}$  in Figure 7) where the  $G''$  is minimum. Alternatively, the average molecular weight between consecutive cross-links ( $M_c \approx \rho RT/G_0$ ) is estimated to be 1700 kg/mol, which is much larger than the molecular weight of an arm of the Star PLA. This suggests that a large number of star arms do not participate in the formation of the percolating network and that the elastically active strands contain several star arms and star centers linked together sequentially. It is likely that the dipolar strength of the ions relative to the intrinsic polarity of poly(L-lactide) is in fact low. A likely reason for this is the H-bonding interaction of  $-\text{OH}$  end groups with the carbonyl of the anion, which effectively reduces the dipolar interactions. Such solvation effects of alcoholic  $-\text{OH}$  functional groups for ionomers are well-known in the literature.<sup>59–62</sup>

**Effect of Ionic Content and Number of Star Arms.** To understand the effect of ionic content on the overall rheological response, six-arm telechelic Star PLA-ionomers of varying ionic contents were synthesized by changing the reaction time for the acidification reaction (step 2). The number of acid end functional groups per molecule was calculated for each polymer from the  $^1\text{H}$  NMR data as discussed earlier. The acid groups were neutralized using NaH to prepare the ionomers. Figure 8 shows strain sweep data for three Star PLA ionomer samples having average ionic contents of two, three, and four ionic end groups per six-arm star. It can be seen from the figure that the shear moduli increase with increasing ionic content and, simultaneously, the strain characterizing the onset of non-linearity decreases with increasing ionic content. This suggests

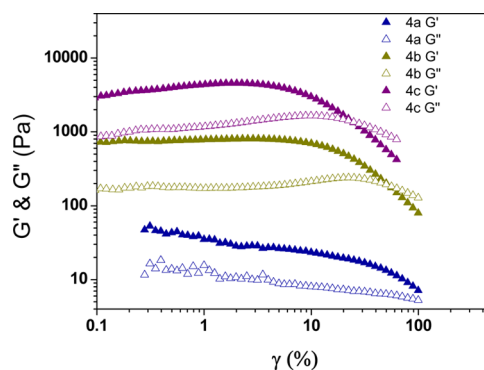


**Figure 8.** Strain sweep data for three different samples of 6-arm star telechelic PLA ionomers having different ionic contents. The sample names in the legend 4a, 4b, and 4c represent the number of ionic groups present per molecule (4a: two ionic end groups; 4b: three ionic end groups; 4c: four ionic end groups).

that the number density of elastically active polymer chains connected to the ionic clusters increased with increase in ionic content.

Finally, we investigated the effect of changing the number of arms of the Star PLA ionomers while keeping constant the molecular weight of star arms. To do so, different multifunctional initiators such as pentaerythritol (PE) and tripentaerythritol (TPE) were used in step 1 of the synthesis procedure. The molecular weight of each arm in the six-arm Star PLA was maintained at approximately 1667 g/mol by choosing the appropriate monomer to initiator ratio for each multifunctional initiator. Thus, the monomer to initiator ratio for the synthesis of four-arm Star PLA taken was 47:1. The overall molecular weight of the four-arm Star PLA was targeted to be 6667 g/mol. Similarly, the monomer to initiator ratio taken for synthesizing an eight-arm Star PLA was 92.6:1. The overall molecular weight of the eight-arm star molecule was targeted to be 13336 g/mol. The acidification protocol (step 2) and the neutralization protocol (step 3) for making the four- and eight-arm Star PLA ionomers were exactly similar to that used for making the six-arm Star PLA ionomer discussed in the earlier section. Detailed structural elucidation of these ionomer was done at each step of synthesis, similar to the six-arm Star PLA ionomers (4). The extent of acidification in the four-arm and eight-arm Star PLA was close to 100%, and the acid end groups were further neutralized to make the Star PLA ionomers. The strain sweep data for the Star PLA ionomers with varying number of arms is shown in Figure 9. For the sake of fair comparison, the rheological data for one of the six-arm Star PLA ionomer batches in which the acidification extent was found to be the highest (nearly 5 of the 6  $-\text{OH}$  end groups per molecule were converted to acid) is shown in Figure 9 along with the data for the four-arm and eight-arm Star PLA ionomers. It can be seen that the viscoelastic moduli increased and the linear region decreased with increase in the number of arms.

The rheology data provide useful information about the microstructure of the Star PLA ionomer melt. The plateau modulus values indicate that the effective molecular weight of a network strand is greater than the arm molecular weight by several orders of magnitude, implying that large numbers of stars have to interconnect to form the network. Based on this information, the microstructure of the star telechelic PLA ionomer melt is schematically represented in Figure 10, where

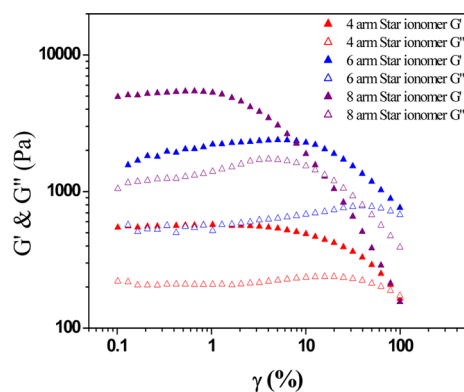


**Figure 9.** Strain sweep for star telechelic PLA ionomers with varying number of arms. The sample names are given as number of arms present in the molecule.

one can see unassociated stars, local aggregates of associated stars, and a loose percolating network formed by a large number of interconnected stars.

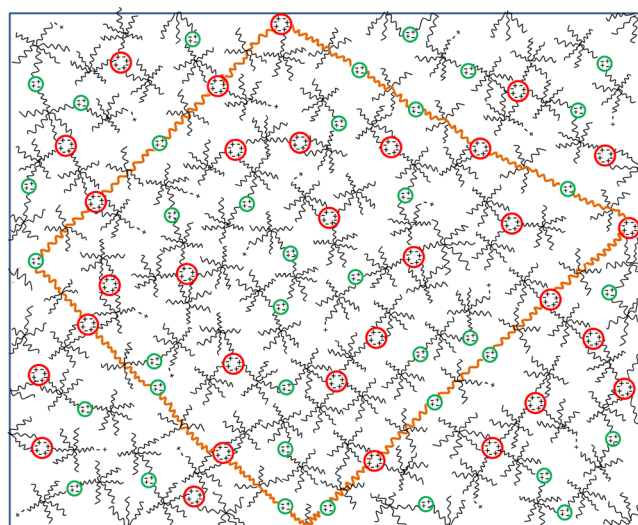


Figure 10. Schematic of star telechelic poly(L-lactide) ionomer melt microstructure.

## CONCLUSIONS

In the present work we have demonstrated the synthesis of star telechelic poly(L-lactide) ionomers through a three-step protocol. The ionomers were characterized using NMR and FTIR to elucidate their molecular structure. The degree of crystallinity of the star ionomers was found to be lower than that of the precursor star polymers. The star ionomers showed two glass transition temperatures: one close to the precursor polymer and the other higher than the precursor polymer. These thermal attributes corroborate the hindered chain mobility of the star ionomers chains. Rheological measurements showed a dramatic increase in the elasticity of ionomer melts relative to that of Star PLA precursor melts. The star ionomer melts were predominantly elastic ( $G' > G''$ , large relaxation time) while the Star PLA precursor melts were predominantly

viscous ( $G'' > G'$ , short relaxation time). The viscoelastic properties of the star telechelic PLA ionomers could be modulated in a facile manner by varying the number of ionic groups per star. The rheological data provide direct support to the existence of a network structure in the ionomer melt. Interestingly, the cross-link density of the network as estimated from the plateau modulus is found to be quite low, thereby indicating that several star ionomers must link together sequentially through dipolar interactions to form the elastically active segments of the network. This work demonstrates that if a few ionic groups are introduced in PLA having MW as low as 10000g/mol, the elastic modulus can be increased by at least 2 orders of magnitude. Introducing ionic groups on high MW PLA would make them more amenable to melt processing applications that require increased melt elasticity.

## ASSOCIATED CONTENT

### Supporting Information

The Supporting Information is available free of charge on the ACS Publications website at DOI: 10.1021/acs.macromol.5b01854.

- (1) Modulated DSC scan and (2) DSC scan after melt crystallized Star PLA ionomer sample;
- (3)  $^1\text{H}$  for Star PLA acids (3a–d);
- (4) reaction kinetics for acidification reaction of Star PLA; and
- (5)  $^{13}\text{C}$ NMR for Star PLA and Star PLA acid (PDF)

## AUTHOR INFORMATION

### Corresponding Author

\*E-mail: ak.lele@ncl.res.in.

### Notes

The authors declare no competing financial interest.

## ACKNOWLEDGMENTS

A.K. acknowledges CSIR, New Delhi, for the Senior Research Fellowship (SRF). We would like to acknowledge Dr. Mrs. Idage and Dr. P. P. Wadgaonkar for help with synthesis of Star PLA. The computational facility from the Yuva cluster in CDAC-Pune, India is thankfully acknowledged. S.V. acknowledges NSF-IIA-1037189 and NSF-CBET-1336311 for funding of travel.

## REFERENCES

- (1) Auras, R.; Harte, B.; Selke, S. *Macromol. Biosci.* **2004**, *4*, 835–864.
- (2) Lim, L.-T.; Auras, R.; Rubino, M. *Prog. Polym. Sci.* **2008**, *33*, 820–852.
- (3) Auras, R.; Lim, L.-T.; Selke, S. E. M.; Tsuji, H. *Poly(lactide acid)*; Wiley Series on Polymer Engineering And Technology; 2010.
- (4) Ameli, A.; Jahani, D.; Nofar, M.; Jung, P. U.; Park, C. B. *J. Cell. Plast.* **2013**, *49*, 351–374.
- (5) Drumright, B. R. E.; Gruber, P. R.; Henton, D. E. *Adv. Mater.* **2000**, *12*, 1841–1846.
- (6) Pilla, S.; Kim, S. G.; Auer, G. K.; Gong, S.; Park, C. B. *Polym. Eng. Sci.* **2009**, *49*, 1653–1660.
- (7) Samuel, C.; Cayuela, J.; Barakat, I.; Müller, A. J.; Raquez, J.-M.; Dubois, P. *ACS Appl. Mater. Interfaces* **2013**, *5*, 11797–11807.
- (8) Carlson, D.; Dubois, P. *Polym. Eng. Sci.* **1998**, *38*, 311–321.
- (9) Di, Y.; Iannace, S.; Di Maio, E.; Nicolais, L. *Macromol. Mater. Eng.* **2005**, *290*, 1083–1090.
- (10) Liu, J.; Zhang, S.; Zhang, L.; Bai, Y. *Ind. Eng. Chem. Res.* **2012**, *51*, 13670–13679.
- (11) Liu, J.; Lou, L.; Yu, W.; Liao, R.; Li, R.; Zhou, C. *Polymer* **2010**, *51*, 5186–5197.

- (12) Deenadayalan, E.; Lele, A. K.; Balasubramanian, M. *J. Appl. Polym. Sci.* **2009**, *112*, 1391–1398.
- (13) Murariu, M.; Bonnaud, L.; Yoann, P.; Fontaine, G.; Bourbigot, S.; Dubois, P. *Polym. Degrad. Stab.* **2010**, *95*, 374–381.
- (14) Murariu, M.; Dechiefa, A. L.; Bonnauda, L.; Painta, Y.; Gallosb, A.; Fontaine, G.; Bourbigot, S.; Dubois, P. *Polym. Degrad. Stab.* **2010**, *95*, 889–900.
- (15) Iwatake, A.; Nogi, M.; Yano, H. *Compos. Sci. Technol.* **2008**, *68*, 2103–2106.
- (16) Abdul Khalil, H. P. S.; Bhat, A. H.; Yusra, A. F. I. *Carbohydr. Polym.* **2012**, *87*, 963–979.
- (17) Kowalczyk, M.; Piorowska, E.; Kulpinski, P.; Pracella, M. *Composites, Part A* **2011**, *42*, 1509–1514.
- (18) Eisenberg, A.; Kim, J. S. W. *Introduction to Ionomers*, 1st ed. (April 22, 1998); Wiley-Interscience: New York, 1998; p 2.
- (19) Lefelar, J. A.; Weiss, R. A. *Macromolecules* **1984**, *17*, 1145–1148.
- (20) Weiss, R. A.; Lundberg, R. D.; Turner, S. R. *J. Polym. Sci., Polym. Chem. Ed.* **1985**, *23*, 549–568.
- (21) Peiffer, D. G.; Weiss, R. A.; Lundberg, R. D. *J. Polym. Sci., Polym. Phys. Ed.* **1982**, *20*, 1503–1509.
- (22) Register, R. A.; Sen, A.; Weiss, R. A.; Cooper, S. L. *Macromolecules* **1989**, *22*, 2224–2229.
- (23) Weiss, R. A.; Agarwal, P. K. *J. Appl. Polym. Sci.* **1981**, *26*, 449–462.
- (24) Morris, B. A. *J. Plast. Film Sheeting* **2007**, *23*, 97–108.
- (25) Orler, E. B.; Moore, R. B. *Macromolecules* **1994**, *27*, 4774–4780.
- (26) Zhang, L.; Brostowitz, N. R.; Cavicchi, K. A.; Weiss, R. A. *Macromol. React. Eng.* **2014**, *8*, 81–99.
- (27) Grady, B. P. *Polym. Eng. Sci.* **2008**, *48*, 1029–1051.
- (28) Eisenberg, A. *Macromolecules* **1971**, *4*, 125–128.
- (29) Hara, M.; Jar, P.; Sauer, J. A. *Polymer* **1991**, *32*, 1622–1626.
- (30) Han, S.-I.; Lee, W. D.; Kim, D. K.; Im, S. S. *Macromol. Rapid Commun.* **2004**, *25*, 753–758.
- (31) Eisenberg, A.; Hird, B.; Moore, R. B. *Macromolecules* **1990**, *23*, 4098–4107.
- (32) Dolog, R.; Weiss, R. A. *Macromolecules* **2013**, *46*, 7845–7852.
- (33) Orler, E. B.; Yontz, D. J.; Moore, R. B. *Macromolecules* **1993**, *26*, 5157–5160.
- (34) Varley, R. J.; van der Zwaag, S. *Polym. Test.* **2008**, *27*, 11–19.
- (35) Witten, T. A.; Cohen, M. H. *Macromolecules* **1985**, *18*, 1915–1918.
- (36) Lundberg, R. D.; Duvdevani, I. *Shear-Thickening Behavior of Ionomers and Their Complexes* **1991**, *462*, 155–175.
- (37) Colby, R.; Zheng, X.; Rafailovich, M.; Sokolov, J.; Peiffer, D.; Schwarz, S.; Strzhemechny, Y.; Nguyen, D. *Phys. Rev. Lett.* **1998**, *81*, 3876–3879.
- (38) Vanhoorne, P.; Register, R. A. *Macromolecules* **1996**, *29*, 598–604.
- (39) Nishioka, A.; Takahashi, T.; Masubuchi, Y.; Takimoto, J.; Koyama, K. *J. Rheol. (Melville, NY, U. S.)* **2002**, *46*, 1325.
- (40) Nishio, M.; Nishioka, A.; Taniguchi, T.; Koyama, K. *Polymer* **2005**, *46*, 261–266.
- (41) Weiss, R. A.; Zhao, H. *J. Rheol.* **2009**, *53*, 191–213.
- (42) Greener, J.; Gillmor, J. R.; Daly, R. C. *Macromolecules* **1993**, *26*, 6416–6424.
- (43) Weiss, R. A.; Yu, W. *Macromolecules* **2007**, *40*, 3640–3643.
- (44) Weiss, R. A.; Fitzgerald, J. J.; Kim, D. *Macromolecules* **1991**, *24*, 1064–1070.
- (45) Stadler, F. J.; Pyckhout-Hintzen, W.; Schumers, J.-M.; Fustin, C.-A.; Gohy, J.-F.; Bailly, C. *Macromolecules* **2009**, *42*, 6181–6192.
- (46) Qiao, X.; Weiss, R. A. *Macromolecules* **2013**, *46*, 2417–2424.
- (47) Connelly, R. W.; McConkey, R. C.; Noonan, J. M.; Pearson, G. H. *J. Polym. Sci., Polym. Phys. Ed.* **1982**, *20*, 259–268.
- (48) Takahashi, T.; Watanabe, J.; Minagawa, K. *Polymer* **1994**, *35*, 5722–5728.
- (49) Ling, G. H.; Wang, Y.; Weiss, R. A. *Macromolecules* **2012**, *45*, 481–490.
- (50) Tant, M. R.; Mauritz, K. A.; Wilkes, G. L., Eds.; *Ionomers: Synthesis, structure, properties and applications*; Springer: 1997.
- (51) Fetters, L. J.; Graessley, W. W.; Hadjichristidis, N.; Kiss, A. D.; Pearson, D. S.; Younghouse, L. B. *Macromolecules* **1988**, *21*, 1644–1653.
- (52) Bagrodia, S.; Mohajer, Y.; Wilkes, G. L.; Storey, R. R.; Kennedy, J. R. *Polym. Bull.* **1983**, *180*, 174–180.
- (53) Bagrodia, S.; Pisipati, R.; Wilkes, G. L. *J. Appl. Polym. Sci.* **1984**, *29*, 3065–3073.
- (54) van Ruymbeke, E.; Vlassopoulos, D.; Mierzwa, M.; Pitsikalis, M.; Hadjichristidis, N.; Pakula, T.; Charalabidis, D. *Macromolecules* **2010**, *43*, 4401–4411.
- (55) Ro, A. J.; Huang, S. J.; Weiss, R. A. *Polymer* **2008**, *49*, 422–431.
- (56) Ro, A. J.; Huang, S. J.; Weiss, R. A. *Polymer* **2009**, *50*, 1134–1143.
- (57) Danko, M.; Libiszowski, J. A. N.; Biela, T.; Wolszczak, M.; Duda, A. *J. Polym. Sci., Part A: Polym. Chem.* **2005**, *43*, 4586–4599.
- (58) Pavia, D. L.; Lampman, G. M.; Kriz, G. S. *Introduction to Spectroscopy*, 4th ed.; 2008.
- (59) Lundberg, R. D.; Company, E. C.; Box, P. *J. Appl. Polym. Sci.* **1986**, *31*, 1843–1858.
- (60) Lundberg, R. D.; Makowski, H. S. *J. Polym. Sci., Polym. Phys. Ed.* **1982**, *20*, 1143–1154.
- (61) Lundberg, R. D. *J. Appl. Polym. Sci.* **1982**, *27*, 4623–4635.
- (62) Fitzgerald, J. J.; Weiss, R. A. *J. Polym. Sci., Part B: Polym. Phys.* **1990**, *28*, 1719–1736.
- (63) Quiram, D. J.; Register, R. A.; Ryan, A. J. *Macromolecules* **1998**, *31*, 1432–1435.
- (64) Kamble, S.; Pandey, A.; Rastogi, S.; Lele, A. *Rheol. Acta* **2013**, *52*, 859–865.